Electrochemical Behavior of Thin Ta_3N_5 Semiconductor Film

Akio Ishikawa,[†] Tsuyoshi Takata,[†] Junko N. Kondo,[†] Michikazu Hara,[†] and Kazunari Domen*[,†,‡]

Chemical Resources Laboratory, Tokyo Institute of Technology, Nagatsuta 4259, Midori-ku, Yokohama 226-8503, Japan, and Core Research for Evolutional Science and Technology, Japan Science and Technology Corporation (CREST, JST), 2-1-13 Higashiueno, Taito-ku, Tokyo 110-0015, Japan

Received: March 18, 2004; In Final Form: May 20, 2004

Tantalum nitride (Ta_3N_5) thin film is investigated as a visible light-driven photoelectrode material. The photoelectrochemical properties of the material are investigated on the basis of cyclic voltammograms and current−time curves, and the conduction and valence band edges of Ta_3N_5 are determined from the photocurrent voltage response. The potentials of the conduction and valence bands are found to be satisfactory for the reduction of H^+ to H_2 and the oxidation of H_2O to O_2. Anodic photocurrent associated with the oxidation of water is obtained under visible-light irradiation, although the Ta_3N_5 itself undergoes simultaneous oxidation. Through sustained photoinduced redox cycling on the Ta_3N_5 electrode in aqueous $Fe(CN)_6^{3-}/Fe(CN)_6^{4-}$ solution, Ta_3N_5 thin film is demonstrated to function as a stable electrode for generating electric current under visible light.

1. Introduction

A number of semiconductors have attracted considerable interest for the conversion of photon energy.[1−3] Photon energy can be converted by semiconductors such as TiO_2, $SrTiO_3$, CdS, and Si into electrical or chemical energy, and some Ti^{4+}-, Nb^{5+}-, and Ta^{5+}-based mixed metal oxides such as $K_2La_2Ti_3O_{10}$, $K_4Nb_6O_{17}$, and $NaTaO_3$ have been successfully applied for photocatalytic overall water splitting as conversion of photon energy into chemical energy.[4−6] However, these photocatalysts are not activated by visible light. The development of a photocatalyst with a visible-light response will therefore contribute significantly to cleaner solar-based energy production.

Recently, a number of (oxy)nitrides of early transition metals such as Ti and Ta have been found to function as photocatalysts with visible-light response.[7−10] As part of the intensive study in this area, the present authors have reported the electronic structures and band positions of TaON and Ta_3N_5.[11] The tops of the valence bands are shifted toward higher potential energies in the order Ta_2O_5 < TaON < Ta_3N_5, whereas the potentials of the conduction band bottoms vary only marginally between −0.3 and −0.5 V (vs NHE at pH 0). The change in the top of the valence band results in smaller band gap energies for these (oxy)nitrides. Through band gap excitations under visible-light irradiation, Ta_3N_5 powder with a band gap of ca. 2 eV evolves H_2 or O_2 from aqueous solutions containing a sacrificial electron donor (methanol) or acceptor (Ag^+) without noticeable degradation.[7] The authors have also developed a method for the preparation of thin films of Ta_3N_5.[11] Considering the stability of Ta_3N_5 as a visible light-driven photocatalyst,[7] the Ta_3N_5/Ta system is expected to be applicable as a visible light-driven photoelectrode. As the electrochemical and photoelectrochemical properties of this thin film have not yet been examined in detail, those properties are investigated in the present study.

2. Experimental Section

2.1. Sample Preparation. Ta_3N_5 thin films (Ta_3N_5/Ta) were prepared by the nitridation of a Ta_2O_5 layer formed on Ta foil (Ta_2O_5/Ta). Ta_3N_5 could not be formed by nitridation of metallic Ta. The Ta_2O_5/Ta precursor was obtained by oxidizing Ta foil ($10 \times 10 \times 0.2$ mm^3, 99%, Nilaco Co.) in air at 823 K for 30 min. The nitridation of Ta_2O_5/Ta was performed in a quartz reaction cell according to the method in the literature.[11] Ta_3N_5/Ta was obtained by exposing a Ta_2O_5/Ta foil to NH_3 at a flow rate of 20 mL/min and a temperature of 1123 K for 4 h. One side of the Ta_3N_5/Ta specimen was polished to expose the Ta metal. A Cu wire was then attached to the polished side of the foil using silver paste. All samples were waterproofed (except for the front surface) using an epoxy resin to prevent current leakage. The samples were characterized by X-ray powder diffraction (XRD; Geigerflex Rad-B, Rigaku; Cu Kα), field-emission scanning electron microscopy (FE-SEM; S-4700, Hitachi), ultraviolet−visible diffuse reflectance spectroscopy (UV−vis DRS; V-560, JASCO), and X-ray photoelectron spectroscopy (XPS; ESCA 3200, Shimadzu).

2.2. Electrochemical Measurement. Cyclic voltammetry was carried out using a conventional electrochemical cell with a Pt counter electrode and an Ag/AgCl reference electrode. A Pyrex cell was used as the electrolytic cell and was filled with 20 mL of electrolyte. The electrolyte was saturated with Ar prior to electrochemical measurements. The photochemical properties were measured under irradiation with visible light ($\lambda \geq 420$ nm) from an Xe lamp (300 W) via a cutoff filter. The gases evolved were analyzed by a thermal conductivity detector (TCD) gas chromatograph. Action spectra were measured under irradiation with a monochromatic lamp. A quartz cell with a flat window was used for action spectra measurement, in which

* To whom correspondence should be addressed. E-mail: kdomen@res.titech.ac.jp.
† Tokyo Institute of Technology.
‡ CREST, JST.

10.1021/jp048802u CCC: $27.50
Published on Web 06/25/2004

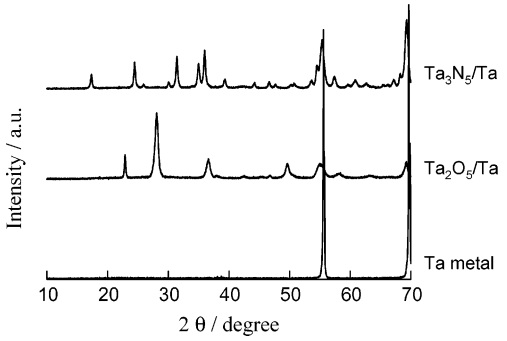

Figure 1. XRD patterns of Ta foil, Ta_2O_5/Ta, and Ta_3N_5/Ta.

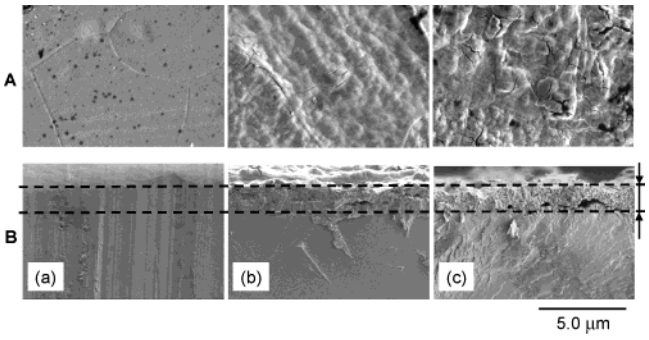

Figure 2. SEM images of (a) Ta foil, (b) Ta_2O_5/Ta, and (c) Ta_3N_5/Ta: (A) surface, (B) cross section.

working, counter, and reference electrodes were set. The number of photons of monochromatic light reaching the electrode surface was measured at each wavelength using an Si photodiode.

The incident monochromatic photon-to-current conversion efficiency (IPCE)[12] is defined as follows.

$$\mathrm{IPCE} = \frac{1250 \times \text{photocurrent density } [\mu\mathrm{A/cm^2}]}{\text{wavelength [nm]} \times \text{photo flux } [\mathrm{W/cm^2}]}$$

3. Results and Discussion

3.1. Characterization of Ta_3N_5 Thin Film. Figure 1 shows the XRD patterns of Ta_2O_5/Ta and Ta_3N_5/Ta. For comparison, the XRD pattern of Ta foil is also shown. All diffraction peaks of Ta_2O_5/Ta and Ta_3N_5/Ta were assigned to those of Ta_2O_5 and Ta_3N_5, respectively, in addition to the substrate material.

Figure 2 shows SEM images of the Ta foil, Ta_2O_5/Ta, and Ta_3N_5/Ta, with corresponding cross sections. The surfaces of Ta_2O_5/Ta and Ta_3N_5/Ta were rougher than that of the original Ta foil and exhibited several cracks. Oxidation or nitridation of the Ta foil resulted in a rough surface morphology. The rough part (ca. 2 μm) of Ta_2O_5/Ta and Ta_3N_5/Ta in the cross-sectional images appears to correspond to Ta_2O_5 and Ta_3N_5 layers. The thickness of the Ta_3N_5 layer was almost the same as that of the Ta_2O_5 layer, indicating that only the oxidized part of the Ta foil was nitrided and that the thickness of the Ta_3N_5 is determined by the thickness of the Ta_2O_5 layer.

3.2. Cyclic Voltammetry of Ta_2O_5 and Ta_3N_5 Electrodes. Cyclic voltammograms of Ta_2O_5/Ta (a) and Ta_3N_5/Ta (b) in 0.1 M H_3PO_4 solution at pH 4 as the supporting electrolyte solution are shown in Figure 3. The pH of the solution was adjusted with KOH. A cathodic current was detected, accompanied by copious bubbling, attributable to hydrogen evolution due to negative polarization of Ta_3N_5/Ta. As seen from the cyclic voltammograms of Ta_2O_5/Ta, the cathodic current under negative polarization was smaller than that for Ta_3N_5/Ta. The onset potential of cathodic current was more negative

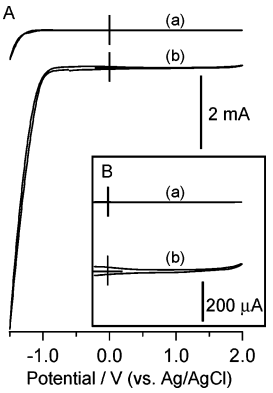

Figure 3. Cyclic voltammograms of (a) Ta_2O_5/Ta and (b) Ta_3N_5/Ta in 0.1 M H_3PO_4 solution at pH 4. Scan rate: 40 mV/s.

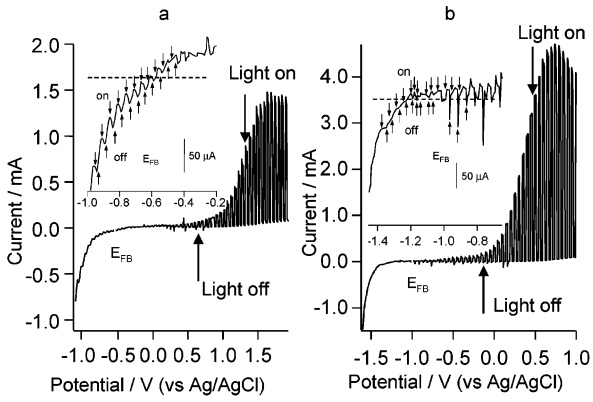

Figure 4. Cyclic voltammograms of Ta_3N_5/Ta electrode in (a) 0.1 M H_3PO_4 (pH 4) and (b) 0.1 M K_2SO_4 (pH 11) under intermittent visible-light irradiation ($\lambda \geq 420$ nm). Scan rate: 5 mV/s.

than that of Ta_3N_5/Ta. The small cathodic current and the negative onset potentials of cathodic currents for Ta_2O_5 appear to be attributable to the low electric conductivity and large overvoltage for H^+-reduction. The anodic current for both Ta_3N_5/Ta and Ta_2O_5/Ta was very small, even at 2.0 V vs Ag/AgCl ($J_D < 50\ \mu\mathrm{A\ cm^{-2}}$), as shown in Figure 3B. The two cyclic voltammograms are essentially identical, with constant values in the potential range from -1.5 to $+2.0$ V vs Ag/AgCl. Therefore, these results indicate that Ta_3N_5/Ta and Ta_2O_5/Ta act as n-type semiconductor electrodes and that the electrochemical properties of Ta_3N_5/Ta and Ta_2O_5/Ta are very similar. The XRD patterns and SEM images of Ta_3N_5/Ta did not reveal any noticeable change due to voltammetry measurements, suggesting that the Ta_3N_5 film does not tend to detach from the substrate during voltage cycling and thus has stable electrochemical properties.

3.3. Electrochemical Properties of Ta_3N_5 Electrode under Visible-Light Irradiation. *3.3.1. Photoelectrolytic Oxidation of Water on Ta_3N_5 Electrode.* The electrochemical properties of Ta_3N_5/Ta electrode under visible-light irradiation were examined using an aqueous solution of 0.1 M H_3PO_4 (pH 4) and 0.1 M K_2SO_4 (pH 11). The pH of the solutions was adjusted with KOH. Figure 4a shows the current density−potential curve for Ta_3N_5 in H_3PO_4 solution as the supporting electrolyte under chopped visible-light irradiation ($\lambda \geq 420$ nm). Anodic photocurrent based on water oxidation was observed at scanning potentials of -0.6 to $+0.1$ V vs Ag/AgCl. At scanning potentials of $+0.1$ to $+1.9$ V vs Ag/AgCl, a small amount of nitrogen evolution based on anodic dissolution of Ta_3N_5 itself was also observed. Therefore, anodic photocurrent observed by positive polarization at more than $+0.1$ V vs Ag/AgCl is probably based

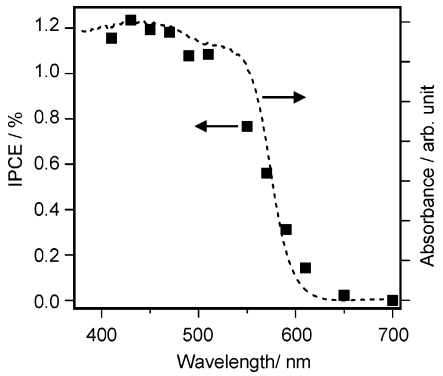

Figure 5. Action spectra of photocurrent generated on Ta_3N_5/Ta electrode in 0.1 M K_2SO_4 solution at pH 11 and −0.1 V under monochromatic visible-light irradiation ($\lambda \geq 420$ nm), and UV−vis diffuse reflectance spectrum of Ta_3N_5 powder (broken line).

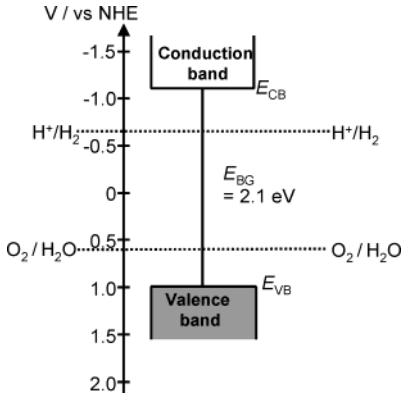

Figure 6. Estimated band positions of Ta_3N_5 in 0.1 M K_2SO_4 solution at pH 11.

on water oxidation and photocorrosion. Figure 4b shows a cyclic voltammogram of the Ta_3N_5/Ta electrode in 0.1 M K_2SO_4 solution under chopped visible-light irradiation ($\lambda \geq 420$ nm). Anodic photocurrent at the Ta_3N_5/Ta electrode appeared in the range −1.0 to +1.0 V vs Ag/AgCl. At more negative than the flat band potential (E_{FB}), the cathodic photocurrent was observed as shown in Figure 4a and b. The cathodic photocurrent appeared to be attributed to the different phenomenon (e.g., thermal excitation) from electrochemical reaction because the cathodic photocurrent was also observed at Ta metal, Ta_2O_5/Ta, and Pt plate. Therefore, the onset potential of anodic photocurrent corresponds to the flat band potential (E_{FB}). The onset potential of photocurrent at pH 11 was ca. −1.0 V vs Ag/AgCl, which is more negative than that obtained at pH 4 (ca. −0.6 V vs Ag/AgCl). The E_{FB} of Ta_3N_5 shifts almost linearly depending on the pH of the electrolyte solution, with a slope of ca. −60 mV/ΔpH. Huygens reported that the E_{FB} of GaN is also a linear function of pH.[18] From ζ potential and interface capacitance measurements, it was found that ζ potential and E_{FB} of Ta_3N_5 depend on pH without the surface oxidation during those measurements.[11] Those results mean that surface ionization is driven by adsorption of H^+ or OH^-. Therefore, the potential energies of Ta_3N_5 vary depending on the pH similarly to those of oxide semiconductor. The intensity of the photocurrent at pH 11 is also higher as compared to that obtained at pH 4. This result is consistent with that for photocatalysis in the powder suspension system,[7] where high activity for O_2 evolution was obtained in alkaline solutions.

3.3.2. Ta_3N_5 Band Positions. Figure 5 shows the action spectra of the Ta_3N_5 electrode measured at a natural bias of −0.1 V vs Ag/AgCl while irradiated with monochromatic light. The UV−vis diffuse reflectance spectrum of Ta_3N_5 powder is also shown for reference. Photocurrent was observed up to 620 nm, and the plots of photocurrent versus wavelength are in good agreement with the diffuse reflectance spectrum of Ta_3N_5. The observed photocurrent was therefore confirmed to occur as a result of band gap transition. E_{BG} is estimated to be 2.1 eV, and E_{FB} of the Ta_3N_5 thin film is estimated to be ca. −1.0 V vs Ag/AgCl at pH 11 (see Figure 4). This E_{FB} is equal to the Fermi level (E_F) of Ta_3N_5. The energy difference between the bottom of the conduction band (E_{CB}) and E_F is assumed to be about 0.3 eV considering that Ta_3N_5 is an insulating n-type semiconductor.[13] The E_{CB} of Ta_3N_5 is estimated to be ca. −1.3 V vs Ag/AgCl at pH 11 (ca. −1.1 V vs NHE), and the E_{VB} of Ta_3N_5 is estimated from the following relationship.

$$E_{VB} = E_{CB} + E_{BG} \quad (1)$$

where E_{BG} represents the band gap energy of Ta_3N_5. On the basis of this relationship, E_{VB} is estimated to be ca. +0.8 V vs Ag/AgCl at pH 11 (ca. +1.0 V vs NHE). The estimated band structure of Ta_3N_5 at pH 11 is illustrated in Figure 6. This band structure is the same as that obtained by interface capacitance measurements and ultraviolet photoelectron spectroscopy (UPS). Reasonable agreement between the results of the two methods is obtained.[11] E_{CB} and E_{VB} are sufficient for the reduction of H^+ to H_2 (−0.6 V vs NHE at pH 11) and the oxidation of water to O_2 (+0.6 V vs NHE at pH 11) via band gap irradiation. However, photoelectrolysis of water carried out at pH 11 and −0.1 V vs Ag/AgCl under visible-light irradiation ($\lambda \geq 420$ nm) gave only low photocurrent densities (ca. 5 μA cm^{-2}), and O_2 evolution was not correctly detectable because of the small amount of evolved O_2. Photoelectrolysis of water at +0.5 V vs Ag/AgCl yielded a lower quantum efficiency (0.03%) of water oxidation on the Ta_3N_5 electrode in the early stage of photoelectrolysis (1 h) as compared to that (10%) achieved by the Ta_3N_5 powder suspension system.[7] In addition, the efficiency of photoelectrolysis decreased with increasing irradiation time. This may be due to degradation of the electrode according to the following decomposition reaction of Ta_3N_5.

$$Ta_3N_5 + 15h^+ + 15OH^- \rightarrow {}^3/_2Ta_2O_5 + {}^5/_2N_2 + {}^{15}/_2H_2O$$

The surface of the Ta_3N_5 thin film was almost entirely oxidized after photoelectrolysis at +0.5 V vs Ag/AgCl for 24 h. These results therefore differ from the stable photocatalysis obtained for the previous powder system.[7] After photoelectrolysis at −0.1 V vs Ag/AgCl, only approximately one-third of the Ta_3N_5 surface was oxidized. Therefore, the instability of Ta_3N_5/Ta is probably due to excessive positive polarization. An excessively positive polarization for a large photocurrent flow is needed for Ta_3N_5/Ta as shown in Figure 4. This implies a high recombination rate in Ta_3N_5 because Ta_3N_5 material is probably a highly defective material. The synthesis of Ta_3N_5/Ta was carried out in a nitridation condition different from that of Ta_3N_5 powder (with a shorter nitridation period (4 h) as compared to that of Ta_3N_5 powder (15 h)). It is considered that the crystallinity of Ta_3N_5/Ta is lower as compared to that of Ta_3N_5 powder. Therefore, the difference in photocatalytic activity and stability between Ta_3N_5/Ta and Ta_3N_5 powder[7] results from the existence of many defects in Ta_3N_5/Ta and the necessity of excessively positive polarization.

On the basis of the present electrochemical study of Ta_3N_5/Ta, the low activity of H_2 evolution on Ta_3N_5 powder can be explained in terms of large band bending at the solid−liquid interface. Because Ta_3N_5 is an n-type semiconductor, a "schottky

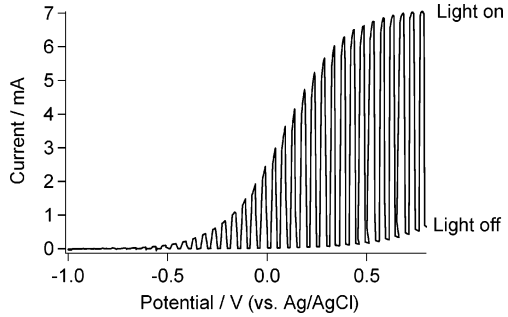

Figure 7. Cyclic voltammogram of Ta_3N_5/Ta electrode in a solution of 0.1 mM $Fe(CN)_6^{3-}$ and 0.1 M $Fe(CN)_6^{4-}$ under chopped visible-light irradiation ($\lambda \geq 420$ nm) at pH 8. Scan rate: 5 mV/s.

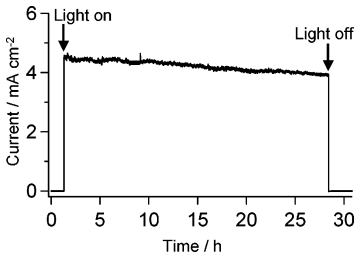

Figure 8. Current−time curve for Ta_3N_5/Ta electrode in solutions of 0.1 mM $Fe(CN)_6^{3-}$ and 0.1 M $Fe(CN)_6^{4-}$ at 0 V vs Pt under visible-light irradiation at pH 8.

barrier" is formed. The barrier may be larger than those formed in oxides that were previously reported as photocatalysts for overall water splitting on account of higher donor concentration in Ta_3N_5. This is because Ta_3N_5 prepared in our present nitridation condition contains many N-vacancies in the crystal. The larger schottky barrier of Ta_3N_5 may hinder prompt electron transfer to H^+ at the surface of catalyst, which is the major problem in performing overall water splitting.

3.3.3. Photoelectrochemical Properties of Ta_3N_5 in Solutions Containing $Fe(CN)_6^{3-}$ and $Fe(CN)_6^{4-}$. As Ta_3N_5 acts as an n-type semiconductor electrode, the application of the Ta_3N_5 electrode to photoelectrochemical cells was examined in an aqueous solution containing 0.1 mM $Fe(CN)_6^{3-}$ and 0.1 M $Fe(CN)_6^{4-}$ complexes.[14,15] Figure 7 show the current density/potential curve for the Ta_3N_5/Ta electrode under chopped visible-light irradiation ($\lambda \geq 420$ nm) in a solution of $Fe(CN)_6^{3-}$/$Fe(CN)_6^{4-}$. Anodic photocurrents were detected on the Ta_3N_5/Ta electrode from −0.7 V. Although the photocurrent density for the photoelectrolysis of water at pH 11 remained between 0.02 and 0.3 mA cm^{-2} below 0 V vs Ag/AgCl, the anodic photocurrent increased remarkably as the electrode was positively polarized from −0.7 V in the presence of $Fe(CN)_6^{3-}$/$Fe(CN)_6^{4-}$ redox media. The maximum photocurrent was obtained in $Fe(CN)_6^{3-}$/$Fe(CN)_6^{4-}$ solution at 0.6 V. These results are probably attributable to a greater activity for the oxidation of $Fe(CN)_6^{4-}$ as compared to the oxidation of water. Figure 8 shows the current−time curve for the Ta_3N_5 electrode at 0 V vs Pt under visible-light irradiation obtained in an electrochemical cell with Ta_3N_5/Ta and Pt electrodes. The current density slowly decreased from 4.5 to 4.0 mA cm^{-2} throughout the experimental period (27 h), attributable to surface oxidation of the Ta_3N_5 film and/or the decomposition of Fe complexes.

3.3.4. Stability of Ta_3N_5 in Aqueous $Fe(CN)_6^{3-}$/$Fe(CN)_6^{4-}$ Solution under Visible-Light Irradiation. The stability of the Ta_3N_5 electrode under visible-light irradiation was evaluated on the basis of surface observations of the Ta_3N_5/Ta electrode by XPS. Figure 9 shows the XPS spectra for Ta_3N_5/Ta samples before and after visible-light irradiation for 27 h, and Table 1

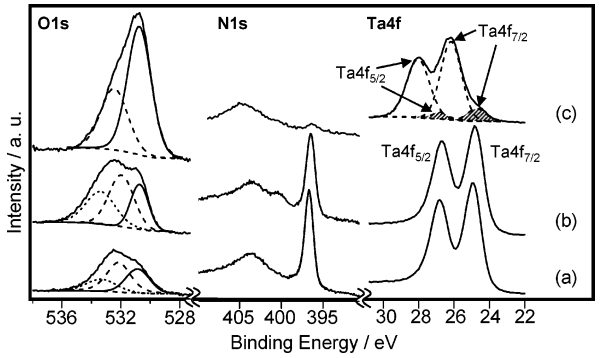

Figure 9. XPS spectra of Ta_3N_5/Ta (a) before and (b,c) after photoelectrolysis, (b) in 0.1 mM $Fe(CN)_6^{3-}$ and 0.1 M $Fe(CN)_6^{4-}$ solution at pH 8 under 0 V vs Pt, and (c) in 0.1 M K_2SO_4 solution at pH 11 under 0.5 V vs Ag/AgCl.

TABLE 1: Surface O/Ta and N/Ta Atomic Ratios of Ta_3N_5 Before and After Photoelectrolysis

	oxidized species	O/Ta	N/TA
Ta_3N_5 thin film		0.3	1.4
after photoelectrolysis for 27 h[a]	$Fe(CN)_6^{4-}$	0.5	1.2
after photoelectrolysis for 24 h[b]	H_2O	2.6	0.1

[a] In 0.1 mM $Fe(CN)_6^{3-}$ and 0.1 M $Fe(CN)_6^{4-}$ solution at pH 8. [b] In 0.1 M K_2SO_4 solution at pH 11.

summarizes the surface atomic ratios of N/Ta and O/Ta for these samples. For comparison, the XPS spectra for Ta_3N_5/Ta after photoelectrolysis for 24 h in the absence of Fe complexes at +0.5 V vs Ag/AgCl are also shown. The surface atomic ratio was estimated from the relative sensitivity factor and the peak areas of Ta 4f, O1s, and N1s orbitals in the XPS spectrum for each sample. The surface atomic ratio of O/Ta was estimated from the O1s peak at 531.0 eV assigned to lattice oxygen.[16] After photoelectrolysis for 24 h in aqueous solution without Fe complexes, the N1s peak disappeared and $Ta4f_{7/2}$ and $Ta4f_{5/2}$ peaks appeared at 26.6 and 28.5 eV. These energy values correspond to Ta^{5+} in Ta_2O_5, as reported in the literature.[16] The surface atomic ratio of O/Ta (2.6) was close to the stoichiometry of Ta_2O_5 (2.5). No significant difference in the binding energies of the Ta4f and N1s peaks was observed after photoelectrolysis for 27 h in an aqueous solution with Fe complexes. However, irradiating the Ta_3N_5 electrode in an aqueous solution with Fe complexes resulted in a small increase in the O1s peak (531.0 eV). The authors have reported that hydrolysis of the surface of Ta_3N_5 thin film in water occurs slowly and almost ceases after 10 days.[17] A total of approximately one-third of the top surface of the Ta_3N_5 is hydrolyzed by immersion in distilled water for any length of time (<20 days). The surface N/Ta atomic ratio as shown in Table 1 is smaller than that of the sample hydrolyzed by immersion in water. It is considered from the XPS data that the observed chemical stability led to the stable electrochemical function of the Ta_3N_5 electrode.

Although Ta_3N_5/Ta was unstable for water oxidation at +0.5 V vs Ag/AgCl, it was stable for the oxidation of $Fe(CN)_6^{4-}$ complexes. The stability of the Ta_3N_5 electrode in an aqueous solution containing Fe complexes appears to be attributable to the high activity for $Fe(CN)_6^{4-}$ oxidation as compared to water oxidation.

4. Conclusion

The electrochemical behavior of Ta_3N_5 thin films was investigated as an n-type semiconductor electrode. An anodic photoinduced ($\lambda \geq 420$ nm) current associated with the oxidation

of water appeared under the application of a potential bias. Action spectra suggested that the observed photocurrent occurred via a band gap transition. Although an anodic photocurrent due to the oxidation of water appeared under visible-light irradiation, the Ta_3N_5/Ta electrode itself underwent oxidation simultaneously. In a solution of $Fe(CN)_6^{3-}/Fe(CN)_6^{4-}$, the photocurrent density was steady at ca. 4 mA cm^{-2} for 27 h, without bias application. No noticeable oxidation of the Ta_3N_5 surface was observed in the aqueous $Fe(CN)_6^{3-}/Fe(CN)_6^{4-}$ system according to XPS. Thus, Ta_3N_5/Ta has been demonstrated to be a suitable electrode material for visible light-driven photochemical cells.

Acknowledgment. This work was supported under the Core Research for Evolutional Science and Technology (CREST) program of the Japan Science and Technology Co. (JST) and The 21st Century COE program of the Ministry of Education, Science, Sports, and Culture of Japan.

References and Notes

(1) Fujisima, A.; Honda, K. *Nature* **1972**, *238*, 37.
(2) O'Regan, B.; Grätzel, M. *Nature* **1991**, *353*, 737.
(3) Domen, K.; Kudo, A.; Ohnishi, T. *J. Catal.* **1986**, *102*, 92.
(4) Takata, T.; Furumi, Y.; Shinohara, K.; Tanaka, A.; Hara, M.; Kondo, J. N.; Domen, K. *Chem. Mater.* **1997**, *9*, 1063.
(5) Kudo, A.; Tanaka, K.; Domen, K.; Maruya, K.; Aika, K.; Onishi, T. *J. Catal.* **1988**, *111*, 67.
(6) Kato, H.; Asakura, K.; Kudo, A. *J. Am. Chem. Soc.* **2003**, *125*, 3082.
(7) Hitoki, G.; Ishikawa, A.; Takata, T.; Kondo, J. N.; Hara, M.; Domen, K. *Chem. Lett.* **2002**, 736.
(8) Hitoki, G.; Takata, T.; Kondo, J. N.; Hara, M.; Kobayashi, H.; Domen, K. *Chem. Commun.* **2002**, 1698.
(9) Kasahara, A.; Nukumizu, K.; Hitoki, G.; Takata, T.; Kondo, J. N.; Hara, M.; Kobayashi, H.; Domen, K. *J. Phys. Chem. A* **2002**, *106*, 6750.
(10) Kasahara, A.; Nukumizu, K.; Takata, T.; Kondo, J. N.; Hara, M.; Kobayashi, H.; Domen, K. *J. Phys. Chem. B* **2003**, *107*, 791.
(11) Chun, W.-J.; Ishikawa, A.; Fujisawa, H.; Takata, T.; Hara, M.; Kawai, M.; Matsumoto, Y.; Domen, K. *J. Phys. Chem. B* **2003**, *107*, 1798.
(12) Nazeeruddium, M. K.; Kay, A.; Rodicio, I.; Humphry-Baker, R.; Muller, E.; Liska, P.; Vlachopoulos, N.; Grätzel, M. *J. Am. Chem. Soc.* **1993**, *115*, 6382.
(13) Matsumoto, Y. *J. Solid State Chem.* **1996**, *126*, 227.
(14) Liu, D.; Kamat, P. V. *J. Phys. Chem.* **1993**, *97*, 10769.
(15) Liu, D.; Kamat, P. V. *J. Electroanal. Chem.* **1993**, *347*, 451.
(16) Kerrec, O.; Devilliers, D.; Groult, H.; Marcus, P. *Mater. Sci. Eng.* **1998**, *B55*, 134.
(17) Hara, M.; Chiba, E.; Ishikawa, A.; Takata, T.; Kondo, J. N.; Domen, K. *J. Phys. Chem. B* **2003**, *107*, 13441.
(18) Huygens, I. M.; Strubbe, K.; Gomes, W. P. *J. Electrochem. Soc.* **2000**, *147*, 1797.